

Towards the Development of Entropy-Based Anomaly Detection in an Astrophysics Simulation

Drew Schmidt
Oak Ridge National Laboratory
Oak Ridge, Tennessee
schmidt@ornl.gov

M. Todd Young
Oak Ridge National Laboratory
Oak Ridge, Tennessee
youngmt1@ornl.gov

Bronson Messer
Oak Ridge National Laboratory
Oak Ridge, Tennessee
bronson@ornl.gov

Michael Matheson
Oak Ridge National Laboratory
Oak Ridge, Tennessee
mathesonma@ornl.gov

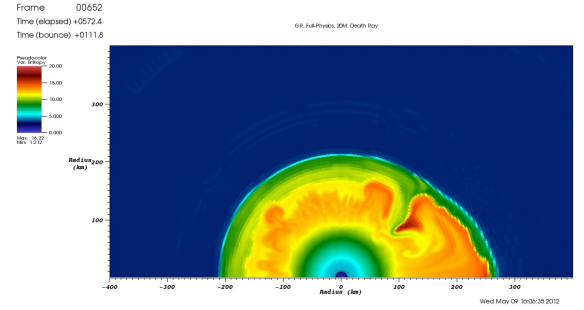
Abstract—The use of AI and ML for scientific applications is currently a very exciting and dynamic field. Much of this excitement for HPC has focused on ML applications whose analysis and classification generate very large numbers of flops. Others seek to replace scientific simulations with data-driven surrogate models. But another important use case lies in the combination application of ML to improve simulation accuracy. To that end, we present an anomaly problem which arises from a core-collapse supernovae simulation. We discuss strategies and early successes in applying anomaly detection techniques from machine learning to this scientific simulation, as well as current challenges and future possibilities.

Index Terms—machine learning, anomaly detection,

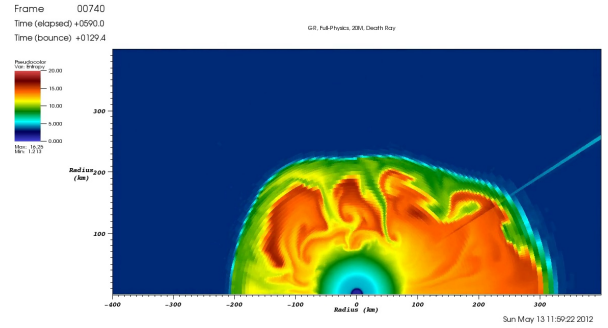
I. INTRODUCTION

Artificial Intelligence (AI) and Machine Learning (ML) have enjoyed a sustained explosion of popularity in recent years. Numerous applications from virtually every field have seen the benefits of AI for science [1]. Much of the excitement in the High Performance Computing (HPC) world has focused on large scale applications of AI methodology for analysis and classification of simulation data that consume gigantic amounts of floating point calculations. Some notable examples of this include [2] and [3]. Others seek to accelerate scientific simulations by replacing part of them with pre-trained deep learning models. In this paper, we instead focus on an attempt at harnessing ML to improve the quality and accuracy of a scientific simulation. Specifically, we seek to build infrastructure which can detect anomalous events during the simulation run and alert the simulation that something has gone wrong.

Even in the most carefully architected software, mistakes occur. These may be simple, easily understood bugs that are quickly patched, or they may be deep sources of consternation that confuse teams for years. Sometimes errors occur that are not even the result of programmer mistakes; most people who have been around software engineers long enough eventually hear jokes about cosmic rays flipping bits in running programs. Of course, more than mere jokes, this can actually happen. It is far less likely to occur in systems with modern ECC RAM, although even then it is possible. Scientific simulations are no



(a) A valid image.



(b) An anomalous image exhibiting the death ray.

Fig. 1: Example images from the simulation. One is a valid image, while the other exhibits the death ray phenomenon.

exception to these rules. They are usually quite large, very complicated, use difficult programming languages, and push the limits of boutique hardware. This compounds any inherent difficulty in finding and fixing software bugs.

We will be examining the outputs of the simulation code CHIMERA [4]. We will discuss the code and its scientific motivation in more depth in Section II-A. For the moment, we motivate only the anomaly problem. Figure 1 shows two

images from this program. These are from a simulation of the collapse and explosion of a massive star in a core-collapse supernova explosion [5]. Figure 1a shows an example of a typical time step from a running simulation, while Figure 1b shows an example of an anomaly. The anomaly is the small line shooting off the edge of the convective interior of the star at roughly 45 degrees from the zenith is jokingly referred to as a “death ray”. It was clear on inspection the death ray was not physical and could not have been the result of any reasonable evolution to that point.

Ideally, the simulation would be able to detect one of these anomalies as it occurs, and then either exit the simulation or perhaps rewind a few time steps to try again. And while it is easy for the human eye to see that something has gone wrong, detecting this from inside the simulation is very challenging. To try to solve this problem, we will turn to techniques from computer vision and data analysis. The goal is to produce a model or framework which can be called by future runs of the simulation as a black box oracle to determine whether or not something has gone wrong. We tackle this with several approaches, each with different strengths and weaknesses.

One aspect of particular interest, the technical aspects of which we explore in Section IV, is the value of the simulation recovering from the detection of an anomaly. The simulation is, in principle, capable of rewinding by reverting to a recent checkpoint. This is in contrast to physical experiments which are often terminated in an unrecoverable state, destroying the experiment. Here, the experiment continues.

Although this work is still early and not fully finalized in a production environment, we have learned some valuable lessons which we believe are of broad interest to anyone working on similar problems of rare event detection for scientific simulation. But before we can begin in earnest, we first discuss the scientific problem at length.

II. BACKGROUND

A. The Scientific Problem

Core-collapse supernovae are among the most energetic events in the Universe, releasing 10^{53} erg of energy on timescales of a few tens of seconds. They produce and disseminate many of the elements heavier than helium, making life as we know it possible. They mark the birth of neutron stars and black holes.

After several million years of evolution and nuclear energy release, a massive star’s core is composed of iron (and similar ‘iron-peak’ elements) from which no further nuclear energy can be released. Above this iron core remains a shell of silicon (Si). At the base of the Si-shell, nuclear burning continues, growing the iron core below. When the mass of the iron core reaches the limiting Chandrasekhar mass, it starts to collapse.

During the collapse, the inner core will become opaque to neutrinos and surpass the density of atomic nuclei ($\gtrsim 2.5 \times 10^{14} \text{ g/cm}^3$) reaching densities where individual nuclei merge together into nuclear matter. Above nuclear density, the nuclear equation of state (EoS) stiffens and the core rebounds like an over-compressed spring, launching a bounce shock from

the newly formed neutron star (a proto-NS; PNS). The shock progresses outward through the rest of the infalling core, heating and dissociating the infalling nuclei to free nucleons and radiating a large burst of neutrinos. Thermal energy removed from the shocked material by neutrinos and nuclear dissociation halts the progress of the shock rendering it a standing accretion shock with a radius of 100–200 km about 50 ms after it is launched. In this accreting state, the inner regions of the star continue to collapse and pass through the shock. The shocked, still infalling matter is dissociated and much of it settles on the PNS. Heating due to accretion onto the PNS drives the emission of neutrinos of all three flavors. Matter heating from neutrino interactions then produces large-scale convective overturn in the shock-heated mantle below the shock. Convection directly beneath the shock serves to markedly alter the state of the matter undergoing reheating via neutrino energy deposition [6]–[11] relative to the spherically symmetric case. This inherently multidimensional effect allows simultaneous downflows that fuel the neutrino luminosities by accretion and upflows that bring energy to the shock.

CHIMERA is a multi-dimensional radiation hydrodynamics code designed to study core-collapse supernovae. The name CHIMERA originates in its combination of three, separate, mature codes. The primary code modules evolve the stellar fluid dynamics (MVH3), the “ray-by-ray” neutrino transport (MGFLD-TRANS), and the thermonuclear kinetics (XNet). These three “heads” are augmented by a sophisticated equation of state for nuclear matter. Hydrodynamics are evolved using a dimensionally split, piecewise parabolic method (PPM) — a version of the publicly available astrophysics PPMLR hydrodynamics code VH1. Self-gravity is computed via multipole expansion in spherical harmonics. Spherical symmetric corrections to gravity for GR replace the non-GR (Newtonian) monopole ($\ell = 0$) term.

In the lower density regions outside the Fe-core, physical conditions require the use of a nuclear network to evolve the time-dependent abundances of nuclei. The nuclear network incorporated into CHIMERA is the publicly available nuclear network code XNet. XNet solves, for each non-equilibrium zone, a coupled system of non-linear ODEs (one for each nuclear species) for the time evolution of the nuclear abundances.

Transport of neutrinos is computed via multi-energy angular moments of the neutrino distribution function in a multi-group, flux-limited diffusion approximation (MGFLD). The neutrino–matter interactions are a modern set that include scattering on electrons and free nucleons with energy exchange, emission and absorption on free nucleons and an ensemble of nuclei in NSE, and neutrino–anti-neutrino pair emission from nucleon–nucleon bremsstrahlung and e^+e^- -annihilation.

CHIMERA has been used on large supercomputer platforms for the past 15 years. Typical runtimes to complete a simulation starting from initial core collapse to 3 seconds of physical time post-bounce have only become possible in 3D over the past few years. Even then, a typical CHIMERA simulation requires hundreds to thousands of compute cores for wallclock

times of months (including queueing times and true runtime) to evolve the first seconds of an explosion. Because of this expense, close attention must be paid to each simulation during the entire run, as any errors that do not halt execution can lead to significant waste of resources.

B. Mapping The Simulation to Images

The CHIMERACode incorporates detailed three dimensional hydrodynamics, a neutron reaction network, neutrino transport, and other physics that are necessary to model core-collapse supernovae. The complex interactions of the various components has made it difficult to determine the root cause of the death ray creation. However, it is possible to restart a simulation from a previously saved timestep and continue execution without encountering a death ray. This suggests that it is possible that a double-bit or multi-bit error has been encountered on the system and may be the cause of the anomaly.

In order to detect the anomaly, we use images created by the VisIt visualization package [12]. The simulation domain is sliced to create a 2D image from the larger domain. The plot creation process naturally handles the mapping from a native polar coordinate simulation with varying grid resolutions to a rectangular image. The entropy variable of the simulation is used and linearly mapped to color by fixing the range by setting a minimum and maximum value for every time step. By fixing the viewport, the slice will be created in a common simulation space. This ensures that consistent images are used for the anomaly detection training and in subsequent simulations for the actual detection for a death ray.

This may seem a bit complicated; and perhaps on some level it is. But recall the key issue illustrated in Figure 1. The problem is easily detected by the human eye, even by someone uninitiated in the daunting field of astrophysics. Yet internally to the simulation, this is an exceedingly difficult problem to detect and correct. So our goal is to develop an AI strategy which can do what the human eye can do. We elucidate this strategy in the following section.

III. METHODOLOGY AND RESULTS

A. Preprocessing

Because our dataset consists of images, a great deal of care and pre-processing specific to image problems must be addressed. However, the core principles outlined here apply beyond image problems.

The images are renderings of the matter entropy, a commonly used diagnostic in supernova simulations. The use of entropy to describe the matter allows clear delineation of the hot, shocked matter above the well-ordered (but, still quite hot) PNS. Our dataset consists of 813 total images, 81 of which are anomalous. This leaves 732 valid images.

Because our data are RGB images, we of course apply the standard pre-processing before transforming them into multi-dimensional arrays. Also, not all of the image is necessary, or perhaps even helpful for training. As can be seen in Figure 1, there is a great deal of extra information, such as the plot

legend and timestamps, as well as lots of white space. For our purposes, we restrict our analysis to only the pixels contained in the intervals [122, 601] for the x coordinates, and [257, 1212] for the y .

After doing standard image pre-processing, our next goal is to extract useful features from the images. To do this, we will use a convolutional neural network (CNN), which are notoriously useful for computer vision. Specifically, we use a ResNet-50 [13] pre-trained on ImageNet [14] as our CNN. To borrow the overly fanciful and evocative language of the NN practitioners, we are essentially borrowing the object recognition capabilities that the network already learned and using them to recognize the important bits of the images in our dataset.

Next is the matter of developing a classifier. This is complicated enough to warrant a careful evaluation, which is the topic of the following subsection. We will use the extracted image features from the pre-trained ResNet-50 with tabular classifiers. One may wonder why we do not use a neural network, such as an autoencoder [15] here. In fact, we tried several such strategies, but with dismally poor results. Therefore, the final pre-processing amounts to reshaping the multi-dimensional array to a matrix of abstract features (even more so than those obtained by the neural network). The matrix will consist of one row per image, giving a dimension of 732×921600 .

B. Model Development Strategies

There are many approaches to model development we could employ. One approach would be to use supervised learning methods. However, this has several drawbacks. For more general anomaly detection strategies, it potentially biases the classifier to particular types of anomalies present only during training because it requires specific labeling of the data.

More specifically to the problem at hand, we essentially only have one anomalous event. Recall, the data consists of 732 valid images, followed by the formation of the death ray. Each image starting from 733 onward is a continuation of the single anomalous event recorded in the data. The death ray expands a bit, experiences some of the same kinds of development as the supernova itself, but ultimately it is a single point of failure. The later images are incorrect, but they are not the demonstrations of failure we seek to discover. This makes models which were developed specifically rare event detection more attractive than general supervised learning classifiers.

Therefore, for our model development, we will employ unsupervised approaches. All of our experiments use one-class SVM [16] and isolation forests [17]. Using SVM is attractive because of its simplicity and its intuitively geometric behavior. The isolation forest is a powerful technique that is conceptually similar to the well-known random forest model in that it too is created from an ensemble of weaker binary classifiers. And like its cousin the random forest, it is known to perform very well for its intended purpose.

Finally, we will use these in two distinct ways: an offline approach and an online approach. For the offline approach,

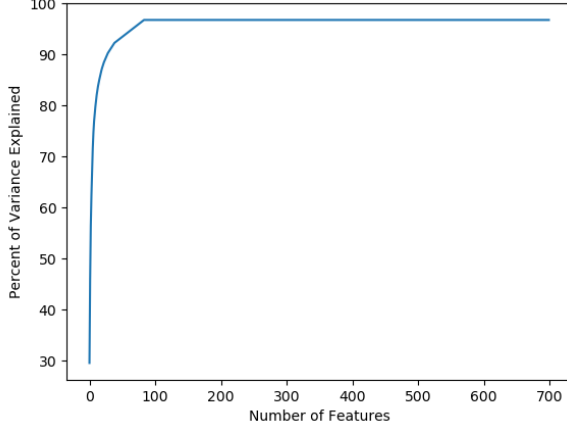


Fig. 2: The percentage of variance explained plotted against the number of PCA rotated features.

we will train on all the data up front as a post hoc process. For the online approach, we will pretend that the full dataset is not actually available to us at training time, as though we were working with the simulation in situ. The development of these strategies is provided in the subsections to follow.

C. Offline Approaches

Because our feature space is so large, we begin by applying principal components analysis (PCA) [18] to position the data into an optimally loaded subspace for developing our classification model. However, since we are only training on the non-anomalous data, we do not need to concern ourselves with the usual issues in principal components regression [19], or consider advanced techniques like sufficient dimension reduction [20].

After applying the typical mean and standard deviation scaling column-by-column (transforming the features into z-scores), we perform PCA. A typical scree plot analysis on a plot such as that in Figure 2 would suggest retaining somewhere on the order of 100 features. However, experimentation with the number of features showed that we achieve uniformly better classifier results as we increase the number of features, up until around 500. For our final model, we retain 512 features, transforming the dataset into a 732×512 matrix. For testing, we use a pool of 40 randomly selected valid images and 20 invalid images.

As noted in the preceding subsection, the models we train on the images are one-class SVM and isolation forest. For each, we optimized the hyperparameters of using Bayesian optimization [21], minimizing the models’ misclassification rates. For the one-class SVM, we use a radial basis kernel function with coefficients $\gamma = 0.001$ and $\nu = 0.01$. For the isolation forest, we used 125 base estimators for the ensemble, $contamination = 0.0$, and $max_sample = 1.0$. After optimizing the model hyperparameters, the SVM achieves 95% accuracy on the test set and the isolation forest gets 100%

accuracy on the test set. The confusion matrix for the SVM’s predictions on the test set is given by Table I. The confusion matrix for the isolation forest’s test set predictions is given by Table II.

		Test Set Anomalous	
		Yes	No
Predicted	Yes	37	3
	No	0	20

TABLE I: SVM Confusion Matrix

		Test Set Anomalous	
		Yes	No
Predicted	Yes	40	0
	No	0	20

TABLE II: Isolation Forest Confusion Matrix

The results of the model performance are summarized in Table III. Both models classify all anomalous images correctly. However, the SVM struggles with the normal, non-anomalous data. The isolation forest on the other hand correctly predicts both normal and anomalous data. Because the one-class SVM struggles significantly more compared to the isolation forest, for now we proceed only with the latter.

Next, we run a series of experiments to test the capacity the trained model has for transfer learning. We begin with using standard image analysis tricks, like mirroring the images. Testing horizontal flips alone, we achieve an overall classifier accuracy of 251/732 on the normal images, and 81/81 of the anomalous. Testing vertical flips (which are impossible for the simulation to actually produce), the model achieves 0/732 on the normal images and 81/81 on the anomalous. Finally, for images which are both vertical and horizontally flipped, the model again scores 0/732 normal images and 81/81 anomalous.

Originally we intended to expand the size of the training set by generating false death rays on existing non-anomalous images. However, this strategy seems to suggest that there is little reason to proceed. Essentially, the model is radically overtraining to the data so that it greatly struggles to detect anything but what it has seen. This is why it is so “good” at detecting anomalies, and almost certainly means that we can not use this trained model on future simulation runs expecting good predictions on the new data. All of this suggests that a different strategy is warranted.

D. Online Approaches

Due to the limitations of the offline approaches in achieving transfer, we proceed with an online approach. Since we actually already have the images, we will pretend that new images are being generated, and develop a new model each time. So it is not truly online, but the strategy could easily be adapted to an actual online environment. It is important to note that we are not, strictly speaking, trying to develop a *model* as the primary outcome, but instead a pool of images which we

Model	Normal	Anomalous	Overall
SVM	662	81	91.4%
Isolation Forest	732	81	100%

TABLE III: Classifier accuracy. Numbers shown in the “Normal” and “Anomalous” columns are counts, i.e. the number of correctly classified images of each type. The “Overall” figure is the weighted classification accuracy.

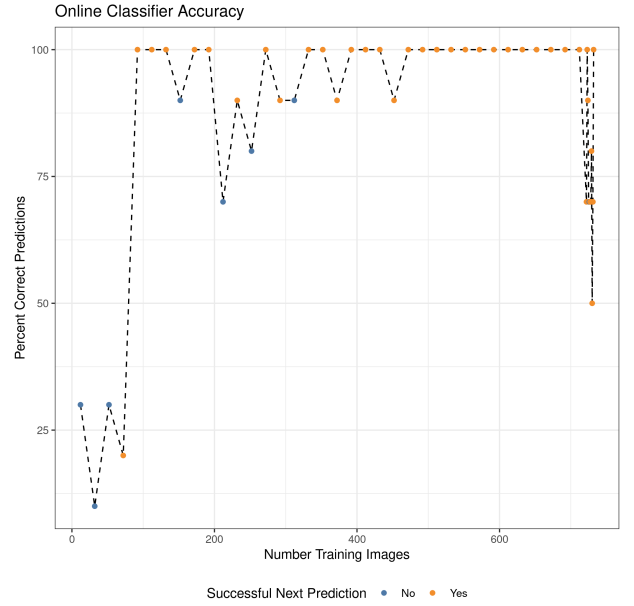
believe are valid. At each step, the model is discarded after making a prediction.

As a baseline, we will start with the model development strategy used in the offline setting, training a new model each time a new image is made available. At that time, we take as a matter of faith that all prior images are valid, train a model like before, and then make a prediction on the new image. Unfortunately, this does not work even a little bit. The models are never able to correctly identify a next image when the image is valid, similar to the problem experienced in the offline setting.

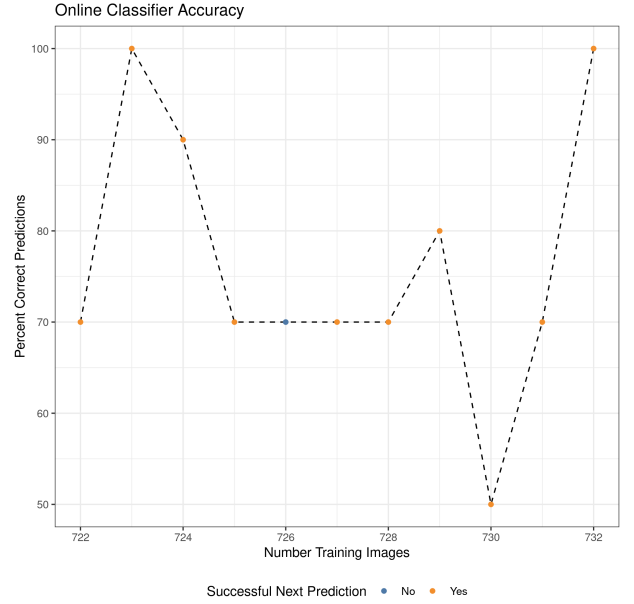
So next, we try developing the models without performing the PCA-based dimension reduction. This radically increases the training time as the dataset grows, which is a serious issue for the true online setting. Nevertheless, proceeding with this shows some promise. Figure 3 shows the results of proceeding in this way. For each model, we test on the last image that the model saw, and find that every time it correctly predicts that image as valid. We then make predictions on the next 9 images, each of which was unseen by the model. This is helpful to ensure that the model is not simply throwing away everything it has not yet seen. However, the only real prediction that matters is for the first image it has not yet seen. In the plot, we color those which are able to make that first true prediction correctly orange, or otherwise blue.

Early on, the classifiers struggle a great deal to make good predictions at all, as can clearly be seen in Figure 3a. But by the time we reach 100 images in the training set, the models score well on their test sets overall. However, we still see many failures on the prediction of the first unseen image until roughly 300 images constitute the training set. After that, they largely disappear. For the models which predict on the anomalous images, shown in clearer detail in Figure 3b, overall we see good performance. Except in one case, specifically the model trained on 725 images, they are all able to correctly predict the first unseen image. This includes the first anomalous image, correctly detected by the model trained on 732 images. And although there is no simple way to demonstrate this in the plot, half of the models were able to correctly detect the first anomalous image in their test set of 9 unseen images. Why the model trained on 725 images fails is not at all clear to us.

As expected, there is a training data accumulation problem with this approach. As we have seen, the initial few models are of poor quality, since they have seen only a handful of snapshots of the simulation. So for spotting early death rays, this is not a good strategy, since we essentially have to build



(a) All model predictions.



(b) Model predictions near and including anomalous images.

Fig. 3: Percent of correct predictions for the series of models from the online training. Each model makes a prediction on the last image it saw plus nine images it has not seen. Models which correctly classify the first unseen image are colored orange, and those which fail are colored blue. The line is dashed for better visibility.

into the decision-making system a distrust of the early models. The best way to overcome this shortcoming is not immediately obvious.

Finally, a few comments about this strategy compared to the offline one above. First, we experimented with SVM models as

before; but also as before, they were seriously outperformed by the isolation forest. In addition, we found no major improvement to the transfer problem by dropping the PCA step in the offline setting. Although it improves somewhat, we find that the online variant shows the most promise. However, the training time is radically more expensive than before, taking hours to fit a single model. And there are not to our knowledge any alternative, high-performance isolation forest packages available which could credibly diminish the computing time to a sufficiently short interval.

IV. INVOKING THE ANOMALY DETECTOR FROM THE SIMULATION

Here, we discuss some strategies for calling the ML framework from the simulation as it produces images. We must do so in such a way that it can inform the simulation if something may have gone wrong. There are several ways in which we could do this, and weighing a few of their pros and cons is warranted.

The simplest option is to simply spawn a new ML process every time a new image is generated. That is, each time the simulation (a C, C++, or Fortran code) produces a new image in need of classification, it will simply spawn a new classifier process via a call to `system()` (with appropriate wrappers in the case of Fortran). The simulation, which may well be a large, distributed code communicating via MPI [22], need only call this on one of its processes. The simulation must wait on hold for the result. But after it is returned to the calling process, that process can then broadcast the result to the remaining processes and act accordingly.

This approach makes the most sense if the run time for the ML process is very short. This aligns with our offline model, where although the run time cost to pre-process many images and perform training is non-trivial, classifying a single image is quite quick. On an ordinary workstation, the total run time to classify a new image is about 5 seconds, including the cost of starting up a new interpreter and loading the necessary libraries and stored data/models.

Our model codes anomalous images as -1 and acceptable ones as 1 . So we merely need to have the interpreter exit with code 0 if the new image is not detected as anomalous (the model prediction is 1), and some non-zero error code otherwise. Putting this into practice, the C code for the sim to call might look as simple as:

```
int classify(char *img_path){
    char cmd[256];
    sprintf(cmd, "/bin/interpreter \
        classify_img.script %
    return system(cmd);
}
```

As noted before, this wrapper is easily made Fortran-compatible via the usual `ISO_C_BINDING`. For this then, the simulation workflow might look something like:

- 1) Simulate time step.
- 2) Generate image, call `classify()` as outline above.

- 3) If the return value is 0 , continue. Otherwise, rewind to the last checkpoint and try again.

If the ≈ 5 second run time for classifying a new image in this set is intolerable, note that roughly half of it is devoted to starting a new interpreter and loading the requisite libraries, data, and models. It is possible to create a persistent process that could be polled by the simulation with, say, a ZeroMQ [23] REQ/REP socket between the calling process of the simulation and the analysis process. The simulation would essentially tell the persistent anomaly detector process that it has a new image at a specified location (communicated over the socket), and the anomaly detector would then evaluate and reply on the same socket.

Neither of these strategies is viable for the online variant due to its radically longer training times. In this case, it would be more reasonable to set aside some compute resources on the supercomputer. That is, some subset of the nodes could be carved out specifically for the processing and training of images. This training can work independently of the sim in an overlapped way. For the first image, the analysis processes would wait. After it is generated, the simulation could proceed to the next time step while the analysis process operates on the first image. Then the simulation generates the second image, proceeds to the third time step, all while the analysis process operates on the second image. And on and on.

Launching this kind of dual application with MPI is straightforward in principle. Say N_1 resources were devoted to the simulation code, while N_2 were devoted to the classifier script. Then one might do something like:

```
mpirun -np ${N1} sim : -np ${N2}
    /bin/interpreter classify_img.script
/sim/img/path
```

In this case, the simulation and the anomaly detector processes each maintain two MPI communicators. One is the main communicator, say `MPI_COMM_WORLD`, and the other is a “local” work communicator only for processes of the same type. This latter communicator is easily constructed via `MPI_COMM_SPLIT`, where say, the simulation uses color 0 and the anomaly detector uses color 1 . In practice this is complicated somewhat by the boutique MPI launcher replacements found on many supercomputers. But the principle remains.

Ideally the analysis process would finish evaluating new images far faster than the simulation of each time step. In this case, deciding when to coordinate the results of the analysis process with the simulation is moot. If the anomaly detection is far slower, then this creates a bottleneck from the point of view of the simulation. That is likely the case for our particular model-building in the online case. Worse, the isolation forest model fitter we use is not scalable even within a single node. This creates the largest hurdle to an actual application of online strategy.

V. CONCLUSIONS AND FUTURE WORK

In this paper, we outlined multiple strategies for developing an entropy-based anomaly detector for a core-collapse supernovae simulation. While the discussion was focused around

our particular scientific dataset, these principles could easily be applied to other scientific domains. We provided two approaches, outlined the advantages and the shortcomings of each, and then closed with strategies for integrating them with the simulation.

Neither approach was fully satisfactory, although for greatly different reasons. We think it may be possible to salvage the offline approach by including more data in the training set. This could be done by generating more images from additional simulation runs, for example. However, in some ways this seems self-defeating. It may be possible to sufficiently expand the dataset using more image transformations. For the online approach, the biggest obstacle to moving this strategy into production is the training time. If this approach is the only viable path forward, then this would necessitate the development of a high-performance isolation forest model fitter, which is a difficult task unto itself.

In a truly online environment, that approach would have access to more information. Namely, we could use the raw data from the simulation as opposed to an image snapshot. It is not guaranteed that this will improve the model accuracy, but it would certainly complicate things regardless.

ACKNOWLEDGEMENTS

This research used resources of the Oak Ridge Leadership Computing Facility at the Oak Ridge National Laboratory, which is supported by the Office of Science of the U.S. Department of Energy under Contract No. DE-AC05-00OR22725.

This manuscript has been authored by UT-Battelle, LLC, under contract DE-AC05-00OR22725 with the US Department of Energy (DOE). The US government retains and the publisher, by accepting the article for publication, acknowledges that the US government retains a nonexclusive, paid-up, irrevocable, worldwide license to publish or reproduce the published form of this manuscript, or allow others to do so, for US government purposes. DOE will provide public access to these results of federally sponsored research in accordance with the DOE Public Access Plan (<http://energy.gov/downloads/doe-public-access-plan>).

APPENDIX A SOFTWARE ENVIRONMENT

Our ML framework is written in the python programming language [24]. Our package, including code and data, is available at <https://code.ornl.gov/va8/autoencoder>. We use python for easiest access to the various Deep Learning frameworks for extracting ResNet features, namely Tensorflow [25], keras [26], and pytorch [27]. We also use keras, as well as Numpy [28], for much of the image pre-processing. We use Scikit-learn [29] to apply PCA, as well as in fitting the SVM and Isolation Forest models. The Bayesian Optimization was performed by the scikit-optimize package [30]. It is worth noting that none of the analysis in Section III relies on features native or exclusive to any particular programming language or package. Finally, we note the package versions used during model development:

- python 3.8.2
- keras 2.4.0
- numpy 1.17.4
- Scikit-learn 0.22.2.post1
- scikit-optimize 0.8.1
- tensorflow 2.3.0

REFERENCES

- [1] R. Stevens, V. Taylor, J. Nichols, A. B. Maccabe, K. Yelick, and D. Brown, “Ai for science,” Argonne National Lab.(ANL), Argonne, IL (United States), Tech. Rep., 2020.
- [2] T. Kurth, S. Treichler, J. Romero, M. Mudigonda, N. Luehr, E. Phillips, A. Mahesh, M. Matheson, J. Deslippe, M. Fatica, *et al.*, “Exascale deep learning for climate analytics,” in *SC18: International Conference for High Performance Computing, Networking, Storage and Analysis*, IEEE, 2018, pp. 649–660.
- [3] N. Laanait, J. Romero, J. Yin, M. T. Young, S. Treichler, V. Starchenko, A. Borisevich, A. Sergeev, and M. Matheson, “Exascale deep learning for scientific inverse problems,” *ArXiv preprint arXiv:1909.11150*, 2019.
- [4] O. Messer, S. Bruenn, J. Blondin, W. Hix, A. Mezzacappa, and C. Dirk, “Petascale supernova simulation with chimera,” in *Journal of Physics: Conference Series*, IOP Publishing, vol. 78, 2007, p. 012049.
- [5] S. W. Bruenn, J. M. Blondin, W. R. Hix, E. J. Lentz, O. E. B. Messer, A. Mezzacappa, E. Endeve, J. A. Harris, P. Marronetti, R. D. Budiardja, M. A. Chertkow, and C.-T. Lee, “Chimera: A massively parallel code for core-collapse supernova simulations,” *The Astrophysical Journal Supplement Series*, vol. 248, no. 1, p. 11, Apr. 2020. DOI: 10.3847/1538-4365/ab7aff.
- [6] M. Herant, W. Benz, W. R. Hix, C. L. Fryer, and S. A. Colgate, “Inside the supernova: A powerful convective engine,” *ApJ*, vol. 435, pp. 339–361, 1994.
- [7] A. Burrows, J. Hayes, and B. A. Fryxell, “On the Nature of Core Collapse Supernovae Explosions,” *ApJ*, vol. 450, pp. 830–850, 1995.
- [8] H.-T. Janka and E. Müller, “Neutrino Heating, Convection, and the Mechanism of Type-II Supernova Explosions,” *A&A*, vol. 306, pp. 167–198, 1996.
- [9] C. L. Fryer and M. S. Warren, “The Collapse of Rotating Massive Stars in Three Dimensions,” *ApJ*, vol. 601, pp. 391–404, 2004.
- [10] R. Buras, M. Rampp, H.-T. Janka, and K. Kifonidis, “Two-dimensional hydrodynamic core-collapse supernova simulations with spectral neutrino transport. I. Numerical method and results for a 15 M_{\odot} star,” *A&A*, vol. 447, pp. 1049–1092, 2006.
- [11] S. W. Bruenn, C. J. Dirk, A. Mezzacappa, J. C. Hayes, J. M. Blondin, W. R. Hix, and O. E. B. Messer, “Modeling Core Collapse Supernovae in 2 and 3 dimensions with spectral neutrino transport,” *J. Phys.: Conf. Ser.*, vol. 46, pp. 393–402, 2006.

- [12] H. Childs, "Visit: An end-user tool for visualizing and analyzing very large data," 2012.
- [13] K. He, X. Zhang, S. Ren, and J. Sun, "Deep residual learning for image recognition," in *Proceedings of the IEEE conference on computer vision and pattern recognition*, 2016, pp. 770–778.
- [14] J. Deng, W. Dong, R. Socher, L.-J. Li, K. Li, and L. Fei-Fei, "Imagenet: A large-scale hierarchical image database," in *2009 IEEE conference on computer vision and pattern recognition*, Ieee, 2009, pp. 248–255.
- [15] M. A. Kramer, "Nonlinear principal component analysis using autoassociative neural networks," *AIChE journal*, vol. 37, no. 2, pp. 233–243, 1991.
- [16] Y. Chen, X. S. Zhou, and T. S. Huang, "One-class svm for learning in image retrieval," in *Proceedings 2001 International Conference on Image Processing (Cat. No. 01CH37205)*, IEEE, vol. 1, 2001, pp. 34–37.
- [17] F. T. Liu, K. M. Ting, and Z.-H. Zhou, "Isolation forest," in *2008 Eighth IEEE International Conference on Data Mining*, IEEE, 2008, pp. 413–422.
- [18] S. Wold, K. Esbensen, and P. Geladi, "Principal component analysis," *Chemometrics and intelligent laboratory systems*, vol. 2, no. 1-3, pp. 37–52, 1987.
- [19] J. M. Sutter, J. H. Kalivas, and P. M. Lang, "Which principal components to utilize for principal component regression," *Journal of chemometrics*, vol. 6, no. 4, pp. 217–225, 1992.
- [20] R. D. Cook and L. Forzani, "Likelihood-based sufficient dimension reduction," *Journal of the American Statistical Association*, vol. 104, no. 485, pp. 197–208, 2009.
- [21] J. Snoek, H. Larochelle, and R. P. Adams, "Practical bayesian optimization of machine learning algorithms," in *Proceedings of the 25th International Conference on Neural Information Processing Systems - Volume 2*, ser. NIPS'12, Lake Tahoe, Nevada: Curran Associates Inc., 2012, pp. 2951–2959.
- [22] D. W. Walker and J. J. Dongarra, "Mpi: A standard message passing interface," *Supercomputer*, vol. 12, pp. 56–68, 1996.
- [23] P. Hintjens, *Zeromq: Messaging for many applications*. "O'Reilly Media, Inc.", 2013.
- [24] G. Rossum, *Python reference manual*, 1995.
- [25] M. Abadi, P. Barham, J. Chen, Z. Chen, A. Davis, J. Dean, M. Devin, S. Ghemawat, G. Irving, M. Isard, *et al.*, "Tensorflow: A system for large-scale machine learning," in *12th {USENIX} symposium on operating systems design and implementation ({OSDI} 16)*, 2016, pp. 265–283.
- [26] F. Chollet *et al.*, *Keras*, 2015.
- [27] A. Paszke, S. Gross, F. Massa, A. Lerer, J. Bradbury, G. Chanan, T. Killeen, Z. Lin, N. Gimelshein, L. Antiga, *et al.*, "Pytorch: An imperative style, high-performance deep learning library," in *Advances in neural information processing systems*, 2019, pp. 8026–8037.
- [28] T. E. Oliphant, *A guide to numpy*. Trelgol Publishing USA, 2006, vol. 1.
- [29] F. Pedregosa, G. Varoquaux, A. Gramfort, V. Michel, B. Thirion, O. Grisel, M. Blondel, P. Prettenhofer, R. Weiss, V. Dubourg, *et al.*, "Scikit-learn: Machine learning in python," *The Journal of machine Learning research*, vol. 12, pp. 2825–2830, 2011.
- [30] T. Head, MechCoder, G. Louppe, I. Shcherbatyi, fcharas, Z. Vinícius, cmmalone, C. Schröder, nel215, N. Campos, T. Young, S. Cereda, T. Fan, rene-rex, K. (Shi, J. Schwabedal, carlosdanielcsantos, Hvass-Labs, M. Pak, SoManyUsernamesTaken, F. Callaway, L. Estève, L. Besson, M. Cherti, K. Pfannschmidt, F. Linzberger, C. Cauet, A. Gut, A. Mueller, and A. Fabisch, *Scikit-optimize/scikit-optimize: V0.5.2*, version v0.5.2, Mar. 2018. DOI: 10.5281/zenodo.1207017. [Online]. Available: <https://doi.org/10.5281/zenodo.1207017>.